Materials Transactions, Vol. 65, No. 1 (2024) pp. 61 to 70

Kinetics Study of Adsorption Behaviors of Trivalent Metal Ions onto Chelating Resin: Comparison between Scandium(III) and Other Metal Ions

Hiroto Watanabe[1,3,*], Satoshi Asano[2] and Kuniaki Murase[3]

[1]*Niihama Research Laboratories, Sumitomo Metal Mining Co., Ltd., Niihama 792-0002, Japan*
[2]*Research & Development Planning & Administration Dept., Sumitomo Metal Mining Co., Ltd., Tokyo 105-8716, Japan*
[3]*Department of Materials Science and Engineering, Kyoto University, Kyoto 606-8501, Japan*

Scandium (Sc) lacks commercially viable independent deposits and is mainly recovered as a by-product of the smelting of other ores. In the process of recovering nickel from laterite ores, Sc is recovered from leaching solutions. The recovery of Sc requires its efficient separation and purification from other impurities. This study proposes a process for the selective separation and recovery of Sc from other trivalent cations in sulfuric acid solutions using an iminodiacetic acid chelating resin, Diaion™ CR11. The adsorption behaviors of trivalent ions Sc(III), Cr(III), Al(III), and Fe(III) onto CR11 in single- and multiple-metal systems were investigated to determine the appropriate Sc separation conditions. In systems containing single metal ions, pseudo-first-order and pseudo-second-order kinetic models were used to fit the data. Linear and nonlinear methods were used for fitting. The activation energies were calculated from the rate constants at a pH of 2.0 and at three different temperatures of 23°C, 60°C, and 80°C and followed the order: Cr(III) > Fe(III) > Sc(III) > Al(III). In binary systems including Sc(III), the simultaneous adsorption of Sc(III) and other trivalent ions onto CR11 was investigated. Previously adsorbed Sc(III) on CR11 was displaced by the subsequent adsorption of Fe(III) or Cr(III) from the solution. The affinity of the metal ions to iminodiacetic acid and the adsorption reaction rate were critical factors for suitable selective Sc separation, indicating that prior removal of Fe(III) was necessary. Column experiments at 23°C using a synthetic solution without Fe(III) showed that Cr(III) adsorption was suppressed, and that Sc(III) was efficiently adsorbed. Scandium can be efficiently recovered from a solution containing Sc(III) after prior removal of Fe(III) by adsorption at low temperature using CR11.
[doi:10.2320/matertrans.M-M2023813]

(Received May 10, 2023; Accepted October 9, 2023; Published November 6, 2023)

Keywords: *ion exchange, chelating resin, trivalent metal ion, scandium, kinetics, binary system*

1. Introduction

Scandium (Sc) and its compounds have been widely used in various fields such as solid oxide fuel cells, Al–Sc alloys, metal halide lamps, and laser crystals.[1,2] Scandia-stabilized zirconia has very high oxygen-ion conductivity and is used as a highly efficient solid electrolyte in solid oxide fuel cells. Al–Sc alloys with small additions of Sc are characterized by high strength, high corrosion resistance, etc. Sc is an extremely effective element for strengthening Al alloys. Despite these attractive properties, however, Sc is not widely used in the industrial and commercial settings because its supply is insufficient. The average crustal abundance of Sc is approximately 22 ppm.[3] Sc is approximately twice as abundant as, for example, lead or boron, and is by no means a rare element. Most of the Sc, however, is decentralized in the crust, and Sc-rich ores are extremely rare. For example, Sc ores include thortveitite ($(Sc,Y)_2Si_2O_7$) from Norway, Madagascar, and Mozambique, and kolbeckite ($ScPO_4 \cdot 2H_2O$) from Utah in the United States; however, the amount of Sc produced is quite small, and no independent large-scale deposits of Sc are available. Other ores with small amounts of Sc include mafic minerals (pyroxene and hornblende), wolframite, tinstone, beryllite, pomegranite, monazite, columbite, zircon, and albite. Sc is recovered and refined in small quantities as a by-product of smelting other ores, including rare earth ores, uranium ores, tungsten ores, lateritic bauxites, and nickel ores,[2,4–10] with a worldwide production of only 15–25 tons/year in 2021 as scandium oxide.[11]

Currently, solvent extraction[12] and ion-exchange resin methods are used to purify Sc from leachate or leach liquor, which contains large amounts of impurities. When the concentration of Sc in the leachate is low (0.1–0.5 mmol L^{-1}), the ion-exchange resin method is more suitable than the solvent extraction method because it requires smaller equipment. Resins that selectively recover Sc have been studied,[13–18] but none are industrially available.

For example, in the process of recovering nickel from laterite ores by using a high-pressure acid leach (HPAL) process,[19–21] Sc is recovered as a by-product from the sulfuric acidic process solution (i.e., the waste solution after nickel recovery, with a pH of approximately 2) via an ion-exchange resin method. The leaching process for Sc from nickel oxide ore is the same as that for nickel and cobalt, and Sc is present in the pregnant solution as the trivalent cation Sc(III). However, its concentration (0.1–0.5 mmol L^{-1}) is lower than the concentrations of other trivalent cations; Cr(III) has a concentration of 0.7–2 mmol L^{-1}, Al(III) of approximately 100 mmol L^{-1}, and Fe(III) of 15–50 mmol L^{-1}.

In this process, a commercially available iminodiacetic acid chelating resin is used to recover Sc,[22] but the adsorption behavior of Sc(III) onto iminodiacetic acid chelating resins has not been well investigated. Iminodiacetic acid has a higher affinity for trivalent metal ions than for monovalent or divalent metal ions. To recover Sc efficiently, it is crucial to evaluate not only the adsorption behavior of each metal ion onto the ion-exchange resin but also the simultaneous adsorption behaviors of Sc and other trivalent metal ions in coexisting systems. Although several studies have been conducted on the adsorption characteristics of single metal ions, the number of studies on the simultaneous

*Corresponding author, E-mail: hiroto.watanabe.z7@smm-g.com

adsorption behaviors and interactions of two or more metal ions has been increasing.[23–47] Li *et al.* performed a study on the simultaneous adsorption behaviors and interactions of Cu(II) and Pb(II) and Cu(II) and Cd(II) in binary systems using an iminodiacetic acid chelating resin and showed that adsorbed Pb(II) or Cd(II) was displaced by subsequently adsorbed Cu(II) with a higher affinity.[32] Lou *et al.* studied the simultaneous adsorption behavior of solutions containing Cd(II), Cr(III), Cu(II), Ni(II), Pb(II), and Zn(II) using micro/nanofibers with amide oximes as functional groups and found that Cr(III) and Pb(II) were adsorbed by substitution with other adsorbed metal ions.[36] However, no detailed studies have been reported on the simultaneous adsorption behavior of metal ions coexisting with Sc(III).

The purpose of this study is to clarify the single and simultaneous adsorption behaviors of the trivalent metal cations, Sc(III), Cr(III), Al(III), and Fe(III), by the iminodiacetic acid chelating resin, Diaion™ CR11, and to gain insight into appropriate treatment conditions during Sc recovery. Kinetics analyses in the presence of impurities are useful in determining how rare and valuable elements such as Sc can be recovered in the industry. If the supply of Sc increases, materials that reduce energy consumption could become more prevalent.

2. Materials and Methods

2.1 Ion-exchange resin

The iminodiacetic acid-chelating resin, Diaion™ CR11, was purchased from Mitsubishi Chemical Co., which was selected in our previous study.[22] Table 1 lists the characteristics of the ion-exchange resins. The resin was transformed from Na- to H-type by mixing with 2.5 mol L^{-1} sulfuric acid solution for 1 h and then washed with pure water.[22]

2.2 Chemicals

Sulfuric acid solutions containing the metal ions were prepared. Solutions containing Cr(III), Al(III), or Fe(III) ions were prepared by dissolving chromium(III) sulfate hydrate, aluminum sulfate hydrate, or iron(III) sulfate hydrate, respectively, purchased from FUJIFILM Wako Pure Chemical Co. These sulfuric salts were used to limit the anions to SO_4^{2-}. Sulfuric acid solutions containing Sc(III) ions were prepared by oxidative dissolution of 99% pure Sc metal purchased from Kojundo Chemical Laboratory Co. In addition to these reagents, the synthesis solutions were prepared using iron(II) sulfate heptahydrate, nickel(II) sulfate hexahydrate, manganese sulfate pentahydrate, magnesium sulfate heptahydrate, and calcium sulfate dihydrate, which were purchased from FUJIFILM Wako Pure Chemical Corporation. The initial pH values were adjusted for each temperature at which adsorption tests were conducted.

Table 1 Diaion™ CR11 characteristics.

Property	
Type	Chelating resin
Matrix	Styrene-DVB, Highly porous
Functional group	Iminodiacetic acid
Cu adsorption capacity / mol L^{-1}	>0.5
Moisture content (%)	60-66
Mean particle size / mm	0.56
Maximum operating temperature / °C	120 (Na^+), 80 (H^+)

2.3 Batch experiments

For the adsorption tests using single and multiple metal-ion systems, 15 mL (4.6 g) of CR11 resin was added to 300 mL of sulfuric acid solution containing metal ions and stirred with a magnetic stirrer. Adsorption tests were performed at temperatures ranging from 23°C to 80°C. The initial pH values were adjusted to 2.0, which was the same as the pH of the waste solution after nickel recovery in the HPAL process. Our previous study has shown that this pH condition results in good separation of impurities.[22] The initial solutions of the metal ions in the single system were prepared with three different concentrations of 0.17, 1.7, and 17 mmol L^{-1} (mmol dm^{-3}). Meanwhile, the initial concentration of each metal ion in the multiple-metal systems was 17 mmol L^{-1}. The highest initial concentration (17 mmol L^{-1}) was determined based on the estimated adsorption capacity of the CR11 resin. The adsorption experiments were also conducted at concentrations of one-tenth (1.7 mmol L^{-1}) and one-hundredth (0.17 mmol L^{-1}) of the capacity, considering the concentration range of the actual process. After phase separation through a cellulose filter paper with a 1.0-μm pore size, the concentrations of the metal ions in the solutions were determined by inductively coupled plasma optical emission spectroscopy (ICP-OES, Agilent Technologies Co., 5100). The amounts of the metal elements adsorbed q_t (mmol g^{-1}) onto the resin at time t (min) were calculated using eq. (1):

$$q_t = \frac{C_0 - C_t}{m} V \tag{1}$$

where C_0 is the initial metal ion concentration, C_t the metal ion concentration at time t, V the solution volume, and m the mass of the dried resin (g).

The adsorption efficiencies A_b (%) of metal ions were calculated using eq. (2):

$$A_b = \frac{C_0 - C_t}{C_0} \times 100 \tag{2}$$

2.4 Column experiments

15 mL of CR11 resin was packed into a jacketed glass column with an inner diameter of 10 mm. Pure water was added to the column so that the resin was submerged, and water at a predetermined temperature flowed through the jacket to control the temperature at adsorption to 23°C or 60°C. Solutions containing metal ions were fed from the top of the column, and effluent samples were collected from the bottom of the column. The concentrations of metal ions in the effluent were analyzed using ICP-OES. After column experiments were conducted, the amounts of the metal elements adsorbed q_f (mmol g^{-1}) onto the resin were analyzed using microwave-assisted digestion and ICP-OES. The adsorption efficiencies A_c (%) of metal ions were calculated using eq. (3):

$$A_c = \frac{q_f W}{C_0 V} \times 100 \quad (3)$$

where W is the resin weight.

2.5 Kinetics of adsorption

The pseudo-first-order rate equation (PFORE) and pseudo-second-order rate equation (PSORE) have been applied for the kinetic quantification of adsorption reactions. PFORE was first proposed by Lagergren.[48] PSORE was introduced in the 1980s.[49,50] Ho *et al.* analyzed several previous studies and showed that many experimental results correlated better with PSORE than with PFORE.[51] Accordingly, PSORE has been applied in many studies. However, Simonin pointed out that the study by Ho *et al.* was not logical because it included experimental data at equilibrium for analysis and classified the results into those that conform to the PFORE, PSORE, or neither of them, based on analyzing the experimental data before equilibrium was reached.[52] Although these kinetic equations are empirical expressions for the chemical reaction of adsorption, some researchers have attempted to derive them from the Langmuir kinetic model. Azizian derived the PFORE under high concentration of adsorbate in solution and the PSORE under low concentrations,[53] Zhang pointed out that systems with higher initial adsorbate concentrations and lower adsorbent dosages, or with lower initial adsorbate concentration and higher adsorbent dosages, were more likely to be described by the PFORE model, while systems with a closer match between the adsorbent capacity and the amount of adsorbate were more suitable, as described by the PSORE model.[54]

The PFORE is expressed by eq. (4):

$$\frac{dq_t}{dt} = k_1(q_e - q_t) \quad (4)$$

where q_e (mmol g^{-1}) is the amount of adsorbate uptake per mass of adsorbent at equilibrium and k_1 (min^{-1}) is the rate constant of PFORE. Equation (4) can be transformed into eqs. (5) and (6) as follows:

$$q_t = q_e\{1 - \exp(-k_1 t)\} \quad (5)$$

$$\log(q_e - q_t) = \log q_e - \frac{k_1 t}{2.303} \quad (6)$$

The PSORE is expressed by eq. (6).

$$\frac{dq_t}{dt} = k_2(q_e - q_t)^2 \quad (7)$$

where k_2 (g mmol^{-1} min^{-1}) is the rate constant of the PSORE. Equation (7) can be transformed into eqs. (8) and (9) as follows:

$$q_t = \frac{q_e^2 k_2 t}{1 + q_e k_2 t} \quad (8)$$

$$\frac{t}{q_t} = \frac{1}{k_2 q_e^2} + \frac{t}{q_e} \quad (9)$$

Although the parameters of the rate equations were calculated using the linear method shown in eqs. (6) and (9), the application of the nonlinear method has recently been recommended by several researchers.[55–58] Furthermore, the calculation of the chi-square (χ^2, eq. (10)) value is recommended in addition to the calculation of the coefficient of determination (R^2, eq. (11)) for the nonlinear method to identify the best-fit model. If the data obtained using the model were similar to the experimental data, χ^2 would be close to zero. High values of χ^2 indicate a high bias between the experimental results and the model. The evaluation in this study was conducted in accordance with these criteria.

$$\chi^2 = \sum \frac{(q_{e,\mathrm{exp}} - q_{e,\mathrm{cal}})^2}{q_{e,\mathrm{cal}}} \quad (10)$$

$$R^2 = 1 - \frac{\sum (q_{e,\mathrm{exp}} - q_{e,\mathrm{cal}})^2}{\sum (q_{e,\mathrm{exp}} - q_{e,\mathrm{mean}})^2} \quad (11)$$

3. Results and Discussion

3.1 Batch experiments

3.1.1 Adsorption in single systems

The kinetics of adsorption from a single solution with an initial C_0 of 17 mmol L^{-1} is shown in Fig. 1. The amount of adsorption increased with an increase in temperature. The

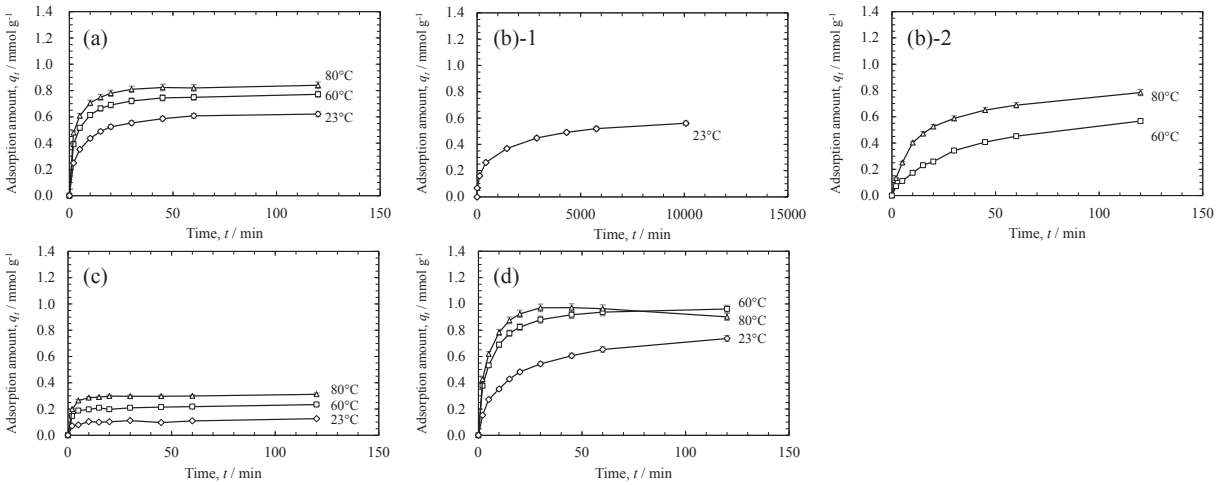

Fig. 1 Effects of time on adsorption of (a) Sc(III), (b)-1,2 Cr(III), (c) Al(III), and (d) Fe(III) adsorption from the single solution with an initial concentration of $C_0 = 17$ mmol L^{-1} onto CR11 resin at different temperatures.

adsorption behaviors of Sc(III) and Fe(III) were similar, and both adsorption amounts of the adsorbate reached equilibrium within a few tens of minutes at temperatures above 60°C. In contrast, the adsorption rate of Cr(III) was low and the amount of Cr(III) adsorbed at 80°C increased even after 120 min. The amount of Al(III) adsorbed was almost constant after 30 min at all the temperatures. The order of the adsorption amounts at 120 min was Fe(III) > Sc(III) > Cr(III) > Al(III).

3.1.2 Kinetics of adsorption

Fittings by PFORE and PSORE were compared by linear and nonlinear regression using the experimental data before equilibrium was reached. Table 2 summarizes the rate constants, R^2 values, and the final pH values of each reaction. Figure 2 shows the experimental data and regression curves for each method for an initial concentration of 17 mmol L^{-1} at 60°C. The linear regression curves for the PFORE showed a large deviation, whereas the other regression curves were consistent with the experimental data. When the nonlinear method was used, the vertical axes of both PFORE (eq. (5)) and PSORE (eq. (7)) were expressed by q_t (mmol g^{-1}). Therefore, using the nonlinear method, it is possible to compare the values of R^2 and χ^2 directly. The comparisons of R^2 and χ^2 in Table 2 show that the PSORE fits the data better under most conditions, indicating that these adsorption reactions are explained by the PSORE. Metal ions are not only adsorbed on the functional groups, i.e., iminodiacetic acid in this study, on the resin's surface but also on those inside the resin by diffusion. The diffusional mass transfer within the resin is thought to occur through repeated adsorption and desorption between metal ions and functional groups and/or diffusion through gaps in the network of cross-linked structures. Diffusion is affected by the adsorption amount.[59] Therefore, these adsorption reactions are consistent with the PSORE. The rate constant k_2 increased with increasing temperature, except for that of Al(III) (see Fig. A1 of Appendix). In other words, the reaction rate increased with increasing temperature. The rate constant k_2 of Al(III)

Table 2 Comparison of the nonlinear pseudo first and second order rate constants for initial ion concentrations, different metal ion species, and temperatures.

Metal ions	C_0 / mmol L^{-1}	T / °C	Final pH	Pseudo first order (nonlinear)			Pseudo second order (nonlinear)		
				k_1 / min^{-1}	R^2	χ^2	k_2 / g $mmol^{-1}$ min^{-1}	R^2	χ^2
Sc(III)	0.17	23	1.9	7.1×10^{-1}	0.86	6.6×10^{-5}	1.4×10^{2}	0.99	2.9×10^{-6}
		60	1.9	1.1×10^{0}	0.92	7.8×10^{-6}	3.2×10^{2}	1.00	1.6×10^{-7}
		80	1.9	1.4×10^{0}	0.95	1.5×10^{-6}	5.7×10^{2}	1.00	1.4×10^{-7}
	1.7	23	1.9	2.8×10^{-1}	0.89	4.0×10^{-3}	3.7×10^{0}	0.99	3.4×10^{-4}
		60	1.9	6.5×10^{-1}	0.85	9.8×10^{-4}	1.1×10^{1}	0.99	6.7×10^{-5}
		80	1.9	8.0×10^{-1}	0.89	4.0×10^{-4}	1.5×10^{1}	1.00	1.9×10^{-6}
	17	23	1.7	1.9×10^{-1}	0.89	4.0×10^{-2}	4.3×10^{-1}	0.98	6.2×10^{-3}
		60	1.7	3.2×10^{-1}	0.87	2.4×10^{-2}	6.0×10^{-1}	0.99	2.9×10^{-3}
		80	1.7	3.9×10^{-1}	0.85	2.2×10^{-2}	7.0×10^{-1}	0.98	2.5×10^{-3}
Cr(III)	0.17	23	2.0	4.7×10^{-5}	0.77	9.2×10^{-2}	5.2×10^{-2}	0.90	3.8×10^{-2}
		60	1.9	3.3×10^{-2}	0.99	3.5×10^{-4}	2.5×10^{0}	1.00	9.7×10^{-5}
		80	1.9	1.7×10^{-1}	1.00	2.9×10^{-5}	1.3×10^{1}	0.99	3.2×10^{-5}
	1.7	23	1.9	1.9×10^{-4}	0.91	4.2×10^{-1}	2.9×10^{-3}	0.92	3.6×10^{-1}
		60	1.9	2.9×10^{-2}	0.93	3.6×10^{-2}	2.4×10^{-1}	0.95	2.2×10^{-2}
		80	1.9	1.4×10^{-1}	1.00	8.0×10^{-4}	1.2×10^{0}	0.99	4.3×10^{-4}
	17	23	1.8	3.8×10^{-4}	0.57	3.3×10^{-1}	1.5×10^{-3}	0.70	2.0×10^{-1}
		60	1.8	3.4×10^{-2}	0.93	1.3×10^{-1}	6.8×10^{-2}	0.96	6.8×10^{-2}
		80	1.7	5.3×10^{-2}	0.94	1.0×10^{-1}	7.4×10^{-2}	0.98	3.4×10^{-2}
Al(III)	0.17	23	2.0	1.8×10^{-1}	0.90	2.3×10^{-4}	6.9×10^{1}	0.98	3.4×10^{-5}
		60	1.9	3.2×10^{-1}	0.90	1.2×10^{-4}	9.8×10^{1}	0.99	8.7×10^{-6}
		80	1.8	3.5×10^{-1}	0.90	1.4×10^{-4}	8.1×10^{1}	0.99	9.7×10^{-6}
	1.7	23	2.0	3.0×10^{-1}	0.93	4.1×10^{-4}	1.8×10^{1}	0.99	3.9×10^{-5}
		60	1.9	3.2×10^{-1}	0.93	1.1×10^{-3}	7.8×10^{0}	1.00	6.2×10^{-5}
		80	1.9	3.7×10^{-1}	0.92	1.1×10^{-3}	7.1×10^{0}	1.00	5.2×10^{-5}
	17	23	1.9	4.6×10^{-1}	0.72	4.3×10^{-3}	6.3×10^{0}	0.87	1.9×10^{-3}
		60	1.8	6.1×10^{-1}	0.90	1.6×10^{-3}	5.2×10^{0}	0.95	7.1×10^{-4}
		80	1.7	5.6×10^{-1}	0.98	5.7×10^{-4}	2.8×10^{0}	0.99	2.9×10^{-4}
Fe(III)	0.17	23	2.0	4.6×10^{-1}	0.99	2.0×10^{-5}	6.0×10^{1}	0.99	1.2×10^{-5}
		60	1.9	1.4×10^{0}	0.86	4.9×10^{-6}	5.1×10^{2}	0.98	6.0×10^{-7}
		80	1.9	1.5×10^{0}	0.99	1.7×10^{-7}	7.9×10^{2}	0.93	1.1×10^{-6}
	1.7	23	1.9	2.2×10^{-1}	0.96	2.5×10^{-3}	2.5×10^{0}	1.00	1.3×10^{-4}
		60	1.9	6.8×10^{-1}	0.99	7.7×10^{-5}	9.8×10^{0}	0.98	8.0×10^{-5}
		80	1.8	9.8×10^{-1}	0.99	1.2×10^{-5}	2.1×10^{1}	0.96	6.1×10^{-5}
	17	23	1.6	7.2×10^{-2}	0.94	8.5×10^{-2}	1.1×10^{-1}	0.98	2.0×10^{-2}
		60	1.6	1.8×10^{-1}	0.92	5.5×10^{-2}	2.6×10^{-1}	0.99	7.5×10^{-3}
		80	1.6	2.9×10^{-1}	0.95	1.6×10^{-2}	3.2×10^{-1}	0.99	2.4×10^{-3}

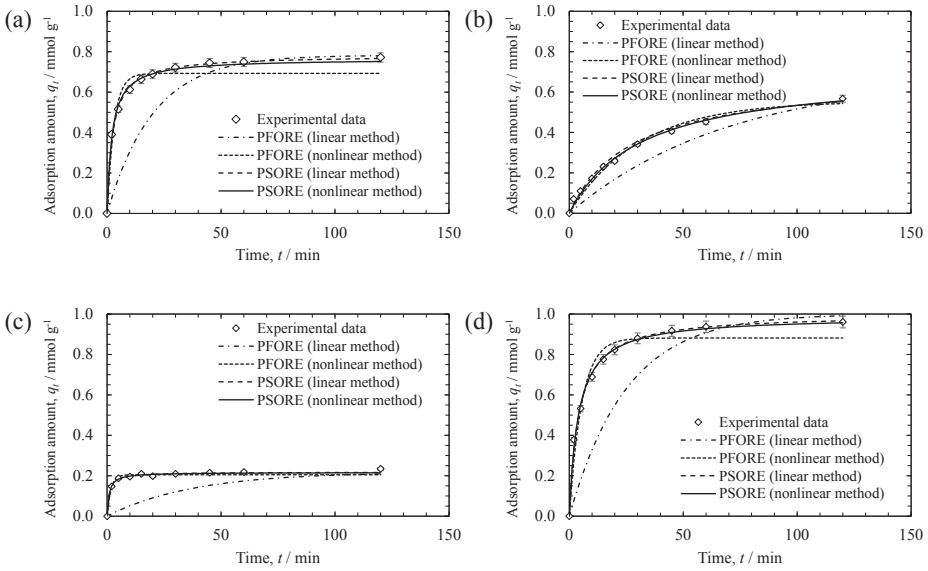

Fig. 2 Model fits of (a) Sc(III), (b) Cr(III), (c) Al(III), and (d) Fe(III) adsorption from the aqueous solution with an initial concentration of $C_0 = 17\,\mathrm{mmol\,L^{-1}}$ onto CR11 resin at 60°C.

may be attributed to its low activation energy, as described below. The rate constant k_2 decreased with increasing initial concentration. The higher the initial concentration, the more the equilibrium adsorption increases due to an increase in the driving force of adsorption. It can be seen from eq. (7) that k_2 decreased with increasing initial concentration. The order of k_2 was Fe(III) $\simeq$ Sc(III) > Cr(III), and that of Al(III) depended on the concentration for reasons unknown. The rate constants for Cr(III) at 23°C were more than two orders of magnitude smaller than those for other elements under the same conditions because the aqua ion of Cr(III) was kinetically inert and ligand exchange was slow.[60–62)]

3.1.3 Activation energies of adsorption

The activation energies of adsorption were estimated using the Arrhenius equation:

$$\ln k_2 = \ln k_0 - \frac{E_a}{RT} \tag{12}$$

where k_2 (g mmol^{-1} min^{-1}) is the rate constant of the PSORE calculated by nonlinear regression, k_0 (g mmol^{-1} min^{-1}) is the temperature independent factor, E_a (J mol^{-1}) is the activation energy of adsorption, R (J K^{-1} mol^{-1}) is the gas constant, and T (K) is the solution temperature. Table 3 lists the activation energies of the adsorption reactions under each condition. The order of activation energies is Cr(III) > Fe(III) > Sc(III) > Al(III), with Cr(III) being the largest, suggesting that lower temperatures are preferred to prevent the adsorption of Cr(III) onto the resin.

3.1.4 Adsorption in binary systems

The simultaneous adsorption behaviors of Sc(III) and Cr(III) were investigated in binary systems containing both metal ions at a concentration of 17 mmol L^{-1}. Figure 3 shows the kinetics of Sc(III) and Cr(III) adsorption from the binary solution at four different temperatures (23, 50, 60, and 80°C). The amounts of Sc(III) and Cr(III) adsorbed after 60 min at 23°C were stable at approximately 0.6 and 0.05 mmol L^{-1}, respectively. The amount of Cr(III) adsorbed at a temperature of 50°C or higher gradually increased after 60 min, whereas

Table 3 Activation energies of each adsorption process.

Metal ions	C_0 / mmol L^{-1}	Pseudo first order (nonlinear)		Pseudo second order (nonlinear)	
		E_a / kJ mol^{-1}	R^2	E_a / kJ mol^{-1}	R^2
Sc(III)	0.17	10.1	1.00	21.2	0.99
	1.7	16.4	0.98	21.6	1.00
	17	11.0	1.00	7.6	1.00
Cr(III)	0.17	128	0.99	85.0	1.00
	1.7	102	0.99	92.6	1.00
	17	79.4	0.95	63.2	0.92
Al(III)	0.17	10.3	0.96	3.4	0.42
	1.7	2.8	0.79	—	—
	17	3.4	0.66	—	—
Fe(III)	0.17	19.3	0.95	40.7	0.98
	1.7	23.1	1.00	32.4	1.00
	17	21.1	1.00	16.3	0.99

that of Sc(III) gradually decreased. Furthermore, as the temperature increased to 60 or 80°C, the amount of Sc(III) adsorbed decreased with increasing Cr(III). In the system containing both Sc(III) and Cr(III), Sc(III) with a larger rate constant was adsorbed first in the initial stage of the adsorption, whereas Cr(III) was adsorbed later, and the adsorption amount of Sc(III) decreased above 50°C; therefore, adsorbed Sc(III) was displaced by subsequently adsorbed Cr(III). Although the adsorption rate of Cr(III) was lower than that of Sc(III), it is reasonable to assume that such a substitution reaction occurred because the stability constant of Cr(III) complexed with iminodiacetic acid was higher than that of Sc(III) (Table 4).

The simultaneous adsorption behaviors of Sc(III) and Al(III) were investigated in binary systems containing both metal ions at a concentration of 17 mmol L^{-1}. Sc(III) was selectively adsorbed, regardless of the adsorption temperature, and the adsorption amount of Al(III) was suppressed to less than 0.1 mmol g^{-1} (see Fig. A2 of Appendix). The low

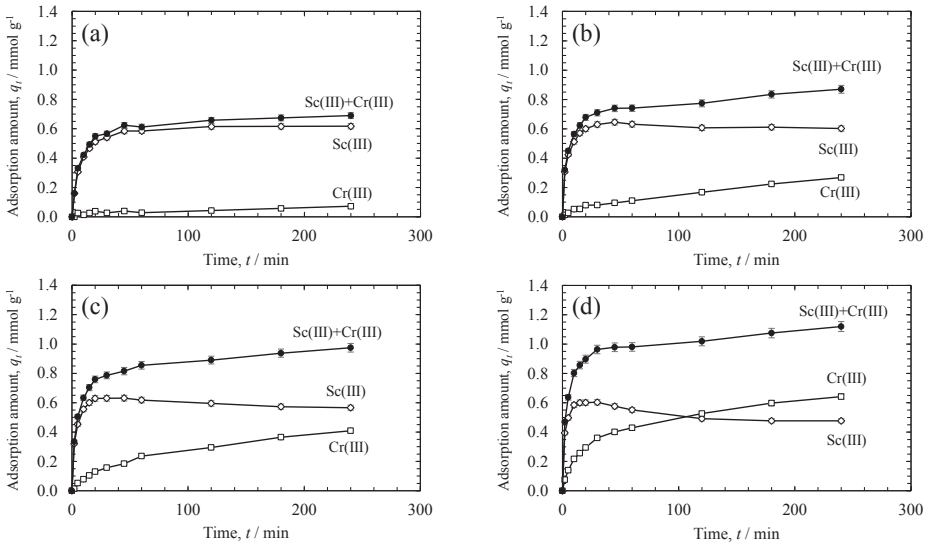

Fig. 3 Effects of time on adsorption of Sc(III) and Cr(III) adsorption from the binary solution onto CR11 resin at (a) 23°C, (b) 50°C, (c) 60°C, and (d) 80°C.

Table 4 Stability constants of the complex of iminodiacetic acid and metal ions.

Metal ions	log K_1	References
Al(III)	8.1	63)
Sc(III)	9.85	64)
Fe(III)	10.72	65)
Cr(III)	10.9	66)

Al(III) adsorption is because the stability constant of Al(III) complexed with iminodiacetic acid is less than one-fiftieth of that of Sc(III).

The simultaneous adsorption behaviors of Sc(III) and Fe(III) were investigated in binary systems containing both metal ions at a concentration of 17 mmol L^{-1}. Figure 4 shows the kinetics of Sc(III) and Fe(III) adsorption from the binary solution at temperatures of 25, 50, and 60°C. The amount of Fe(III) adsorbed increased with increasing adsorption time or temperature and was always superior to that of Sc(III). On the contrary, the amount of Sc(III) adsorbed peaked at approximately 0.4 mmol L^{-1} within 10 to 30 min and then began to decrease. Therefore, the adsorbed Sc(III) ions were displaced by subsequently adsorbed Fe(III). In the case of Cr(III), the complex stability constant of Fe(III) with iminodiacetic acid was higher than that of Sc(III), causing this substitution reaction.

3.1.5 Adsorption in quaternary systems

The simultaneous adsorption behavior of Sc(III), Cr(III), Al(III), and Fe(III) was investigated in a quaternary system containing each metal ion at a concentration of 17 mmol L^{-1}. Figure 5 shows the kinetics of Sc(III), Cr(III), Al(III), and Fe(III) adsorption from the quaternary solution at two different temperatures of 23°C and 60°C. At 23°C, the adsorption of Cr(III) and Al(III) was suppressed to less than 0.1 mmol g^{-1}, and the adsorption behaviors of Sc(III) and Fe(III) were comparable to those in these binary systems. When the temperature was increased to 60°C, the adsorptions of Fe(III) and Cr(III) increased, while that of Sc(III)

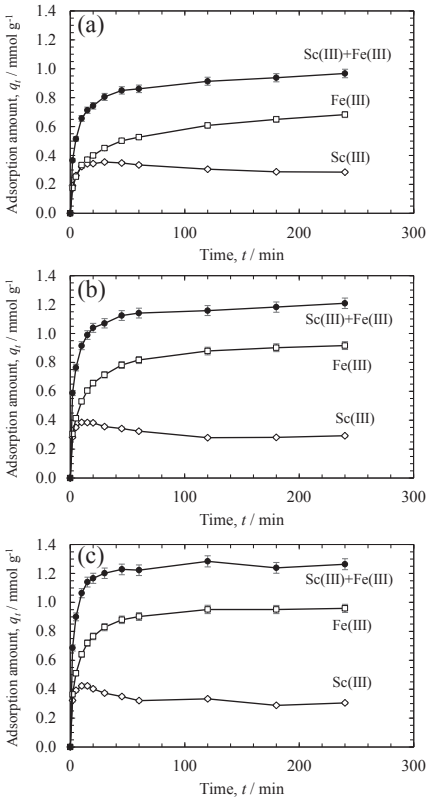

Fig. 4 Effects of time on adsorption of Sc(III) and Fe(III) adsorption from the binary solution onto CR11 resin at (a) 25°C, (b) 50°C, and (c) 60°C.

decreased. The amount of Fe(III) adsorbed was the largest among the four metal ions at all temperatures. The stability constant of Cr(III) complexed with iminodiacetic acid was 1.5 times larger than that of Fe(III), but the rate constant of Fe(III) at 60°C was four times larger than that of Cr(III). Therefore, Fe(III) was preferentially adsorbed and desorbed via the substitution reaction with Cr(III). When using the iminodiacetic acid chelating resin Diaion™ CR11, Fe(III) is preferentially adsorbed under all conditions; therefore,

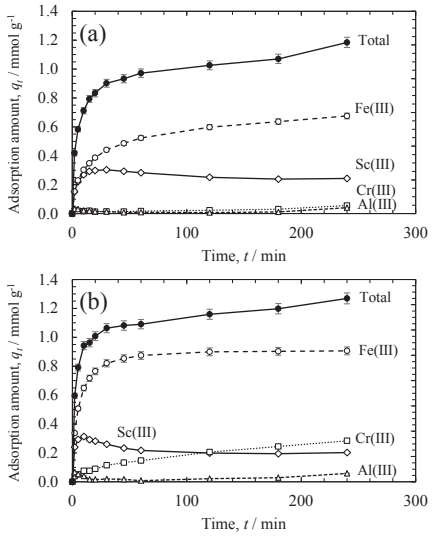

Fig. 5 Effects of time on adsorption of Sc(III), Cr(III), Al(III) and Fe(III) adsorption from the quaternary solution onto CR11 resin at (a) 23°C and (b) 60°C.

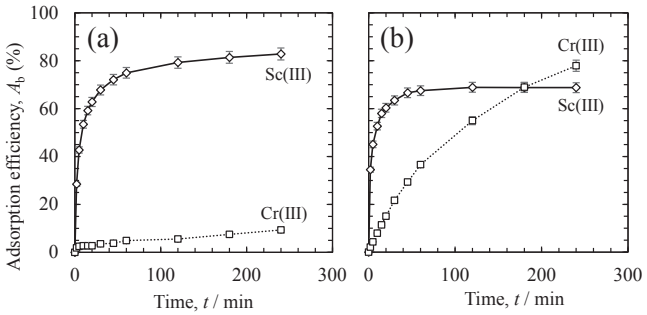

Fig. 6 Adsorption efficiencies of Sc(III) and Cr(III) from the synthetic solution onto CR11 resin at (a) 23°C and (b) 60°C.

removing Fe(III) in advance to recover the Sc component is essential.

These results suggest that the adsorption behaviors are associated with the activation energies and stability constants of metal ions complexed with iminodiacetic acid in the multiple metal-ion systems. In the single system, the amount of Sc(III) adsorbed increased with increasing temperature, whereas in the systems containing both Sc(III) and Cr(III), that amount was higher at 23°C than at 60°C. The results in the binary systems indicate that Cr(III) and Fe(III), which have higher affinities to iminodiacetic acid than Sc(III), can be adsorbed by substitution with adsorbed Sc(III).

3.1.6 Adsorption behavior in synthetic solutions

Because Fe(III) is preferentially adsorbed on CR11 resin over Sc(III), CR11 resin is ineffective for processing solutions containing a large amount of Fe(III). In the HPAL process, the form of Fe ions in the filtrate at approximately a pH of 2 of the sulfurization process that produces mixed sulfide is Fe(II), and the solution contains no Fe(III) ions. The synthetic solutions shown in Table 5 were prepared using the procedure described in our previous study,[22] and the simultaneous adsorption behavior was investigated at temperatures of 23°C and 60°C.

Figures 6 and A3 show the adsorption efficiencies and adsorption amounts, respectively, of Sc(III) and Cr(III) from the synthetic solution at temperatures of 23°C and 60°C. At 23°C, the adsorption efficiencies of Sc(III) and Cr(III) in 240 min were 83% and 9%, respectively, and the amount of Sc(III) adsorbed was higher than that of Cr(III). Sc(III) was preferentially adsorbed at 23°C. At 60°C, these adsorption efficiencies were 69% and 78%, respectively, indicating an increase in the adsorption efficiencies of Cr(III) and a decrease in the adsorption efficiency of Sc(III). The initial adsorption efficiency of Sc(III) was higher than that of Cr(III); however, the opposite was the case at 240 min. The amount of Cr(III) adsorbed was higher than that of Sc(III) after 15 min, and Cr(III) was preferentially adsorbed at 60°C.

The results using synthetic solutions without Fe(III) indicate that Sc(III) was efficiently adsorbed, and, as in the binary and quaternary systems, the amount of Cr(III) adsorbed was more suppressed at 23°C than at 60°C.

3.2 Column experiments

In the actual process, the column was packed with ion-exchange resin and fed with a solution containing the Sc component for adsorption. In the column method, the adsorption reaction starts at the inlet side of the column. The concentration of metal ions in the solutions and the amount adsorbed on the resin change depending on the volume of solution fed and the position in the column from the inlet side to the outlet side. Although qualitative trends can be identified, the adsorption behaviors in the batch experiments reflect the specific circumstances of the column experiments. Adsorption behaviors should be investigated using both column and batch experiments.

In column experiments, the simultaneous adsorption behavior of Sc(III) and impurity metal ions was investigated at 23°C and 60°C using the synthetic solution. A total of 750 mL (bed volume: BV = 50) of the synthetic solution was fed to the column at a flow rate of 1 mL min^{-1} (space velocity: SV = 4 h^{-1}) to examine the adsorption behavior. The concentrations of Sc(III) and Cr(III) in the effluent were different from those in the solution before adsorption, whereas the concentrations of Al(III) and Fe ions were almost the same. Figure 7 shows the breakthrough curves of Sc(III) and Cr(III) at 23°C and 60°C. The Sc leakage rate, which is the ratio of the concentration of Sc(III) in the effluent solution to that of Sc(III) in the solution before adsorption, showed an increasing trend from a BV of approximately 25 at 23°C and 15 at 60°C. Meanwhile, the leakage rate of Cr(III) at 60°C was lower than that at 23°C. The amount of Sc(III) adsorbed decreased at higher

Table 5 Concentration of metal ions and SO_4^{2-} in the synthetic solution after the sulfurization process of HPAL.

Contents	Sc(III)	Cr(III)	Al(III)	Fe(II)	Ni(II)	Mn(II)	Mg(II)	Ca(II)	SO_4^{2-}
C_0 / mmol L^{-1}	0.31	1.7	93	20	0.58	120	280	6.5	560

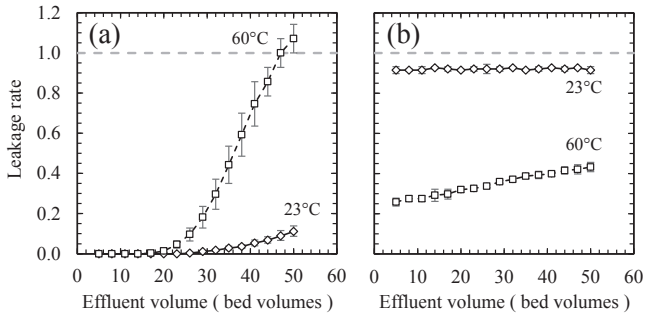

Fig. 7 Breakthrough curves of (a) Sc(III) and (b) Cr(III) adsorption from the synthetic solution onto CR11 resin at 23°C and 60°C.

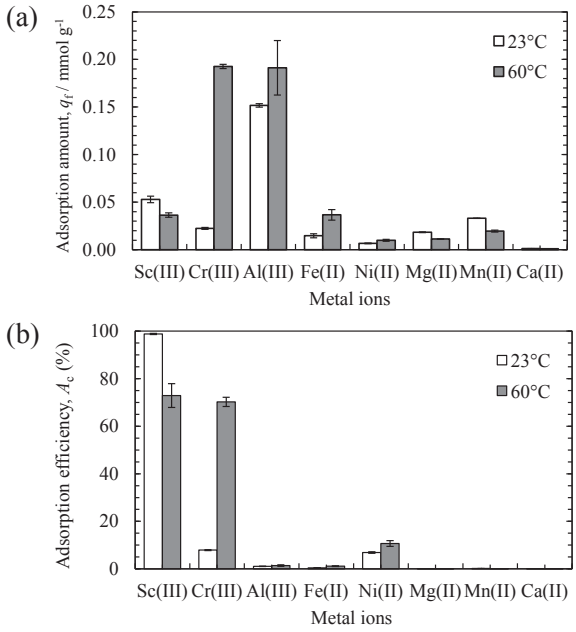

Fig. 8 (a) Adsorption amounts and (b) adsorption efficiencies of metal ions adsorption from the synthetic solution onto CR11 resin after 50 BV at 23°C and 60°C.

temperatures because of the higher amount of Cr(III) adsorbed. The results show a similar trend to those of batch experiments in multiple metal-ion systems containing Sc(III) and Cr(III).

The leakage rate of Sc(III) at 60°C exceeded 1 after a BV value of 47, indicating that the Sc(III) adsorbed onto the resin was subsequently displaced by the adsorption of Cr(III) in the solution, as in the batch experiments (e.g., Fig. 3(c)).

Figures 8(a) and (b) show the adsorption amounts and efficiencies, respectively, of metal ion adsorption from the synthetic solution for a BV of 50 and higher at 23°C and 60°C. At 23°C, the amount of Sc(III) adsorbed was almost 100%. However, the amount of A(III) adsorbed was the highest, at three times that of Sc(III), despite its adsorption efficiency being 1% because its initial concentration was 300 times higher than that of Sc(III). The amounts of other impurities adsorbed were less than the amount of Sc(III). At 60°C, the amount of Sc(III) adsorbed was 30% lower than that at 23°C, and the amount of Cr(III) adsorbed was 8 times higher than that at 23°C. The amount of Fe ions adsorbed was less than that of Sc(III), despite the initial concentration of Fe(II) being 60 times that of Sc(III), because most of the Fe ions were of the type of Fe(II). The adsorption efficiency of Ni(II) was approximately 10%, which was the highest among the divalent metal ions. Al(III) and Ni(II) can be efficiently separated from Sc(III) in the desorption process.[22)]

By using CR11 resin, adsorption at lower temperatures is more efficient for recovering Sc(III) from solutions in which the impurity concentration is higher than the concentration of Sc(III).

4. Conclusions

The adsorption behaviors of the trivalent ions Sc(III), Cr(III), Al(III), and Fe(III), were compared using the iminodiacetic acid-chelating resin Diaion™ CR11. The adsorption behaviors of each metal ion at the initial concentrations of 0.17, 1.7, and 17 mmol L^{-1} and temperatures of 23°C, 60°C, and 80°C were more compatible with the PSORE than with the PFORE. This finding suggests that the amount of adsorbate relative to the capacity of the adsorbent resin is better described by the PSORE. The order of the rate constant k_2 was Fe(III) $\simeq$ Sc(III) > Cr(III), while that of Al(III) depended on the concentration. The order of E_a was Cr(III) $\gg$ Fe(III) > Sc(III) > Al(III).

In a system where Sc(III) coexisted with Cr(III) or Fe(III), Sc(III) adsorbed onto the resin could be subsequently displaced by the adsorption of Cr(III) or Fe(III) in the solution. Substitution between Sc(III) and Cr(III) was promoted at higher temperatures. These behaviors indicate that prior removal of Fe(III) is important for Sc recovery, that adsorption should be carried out at low temperatures to suppress Cr(III) adsorption, and that the reaction time should be controlled appropriately.

Thermodynamic analyses of adsorption and desorption behaviors will be investigated in the future to understand them in more detail.

Acknowledgments

We also thank Tatsuya Higaki and Masako Suekane for their technical assistance.

REFERENCES

1) O. Takeda and T. Okabe: J. MMIJ **137** (2021) 36–44.
2) W. Wang, Y. Pranolo and C.Y. Cheng: Hydrometallurgy **108** (2011) 100–108.
3) R.L. Rudnick and S. Gao: *Treatise on Geochemistry*, (Elsevier Inc., Amsterdam, 2nd ed., 2013) pp. 1–51 (online). http://dx.doi.org/10.1016/B978-0-08-095975-7.00301-6 (accessed 2022-11-19).
4) A.B. Botelho Junior, D.C.R. Espinosa, J. Vaughan and J.A.S. Tenório: Miner. Eng. **172** (2021) 107148.
5) W. Le, S. Kuang, Z. Zhang, G. Wu, Y. Li, C. Liao and W. Liao: Hydrometallurgy **178** (2018) 54–59.
6) H. Nie, Y. Wang, Y. Wang, Z. Zhao, Y. Dong and X. Sun: Hydrometallurgy **175** (2018) 117–123.
7) M.T. Ochsenkühn-Petropoulou, K.S. Hatzilyberis, L.N. Mendrinos and C.E. Salmas: Ind. Eng. Chem. Res. **41** (2002) 5794–5801.
8) X. Zhang, K. Zhou, Y. Wu, Q. Lei, C. Peng and W. Chen: J. Rare Earths **38** (2020) 1322–1329.
9) J. Zhou, S. Ma, Y. Chen, S. Ning, Y. Wei and T. Fujita: Hydrometallurgy **204** (2021) 105724.

10) Z. Zhou, B. Ma, C. Wang, Y. Chen and L. Wang: Process Saf. Environ. Prot. **165** (2022) 161–172.
11) Mineral commodity summaries 2022 (U.S. Geological Survey, 2022) (online). https://doi.org/10.3133/mcs2022.
12) W. Wang and C.Y. Cheng: J. Chem. Technol. Biotechnol. **86** (2011) 1237–1246.
13) H. Cui, J. Chen, H. Li, D. Zou, Y. Liu and Y. Deng: AIChE J. **62** (2016) 2479–2489.
14) J.-Y. Moon, C. Takajo, S. Nishihama and K. Yoshizuka: Solvent Extr. Res. Dev. Jpn. **27** (2020) 91–97.
15) M. Sharaf, W. Yoshida, F. Kubota and M. Goto: J. Chem. Eng. Jpn. **52** (2019) 49–55.
16) N. Van Nguyen, A. Iizuka, E. Shibata and T. Nakamura: Hydrometallurgy **165** (2016) 51–56.
17) Q. Yu, S. Ning, W. Zhang, X. Wang and Y. Wei: Hydrometallurgy **181** (2018) 74–81.
18) L. Zhu, Y. Liu, J. Chen and W. Liu: J. Appl. Polym. Sci. **120** (2011) 3284–3290.
19) Y. Ozaki, M. Imamura and N. Tsuchida: J. MMIJ **131** (2015) 74–81.
20) Y. Ozaki, T.H. Okabe and Y. Kagawa: J. MMIJ **130** (2014) 93–103.
21) N. Tsuchida: J. MMIJ **124** (2008) 549–553.
22) H. Watanabe, J. Hayata, S. Asano and K. Murase: J. MMIJ **138** (2022) 51–59.
23) H. Azad, M. Mohsennia, C. Cheng and A. Amini: J. Environ. Chem. Eng. **9** (2021) 106214.
24) H. Bai, J. Chen, X. Zhou and C. Hu: Korean J. Chem. Eng. **37** (2020) 1926–1932.
25) J.K. Bediako, S. Kim, W. Wei and Y.S. Yun: Int. J. Environ. Sci. Technol. **13** (2016) 875–886.
26) T. Bohli, A. Ouederni and I. Villaescusa: Euro-Mediterr. J. Environ. Integr. **2** (2017) 19.
27) M. Bozorgi, S. Abbasizadeh, F. Samani and S.E. Mousavi: Environ. Sci. Pollut. Res. Int. **25** (2018) 17457–17472.
28) Y. Deng, S. Huang, C. Dong, Z. Meng and X. Wang: Bioresour. Technol. **303** (2020) 122853.
29) H. Guo, S. Zhang, Z. Kou, S. Zhai, W. Ma, Y. Yang and Y. Huang: RSC Adv. **5** (2015) 92885–92892.
30) S. Konishi, K. Saito, S. Furusaki and T. Sugo: J. Membr. Sci. **111** (1996) 1–6.
31) L.F. Koong, K.F. Lam, J. Barford and G. McKay: J. Colloid Interface Sci. **395** (2013) 230–240.
32) B. Li, F. Liu, J. Wang, C. Ling, L. Li, P. Hou, A. Li and Z. Bai: Chem. Eng. J. **195–196** (2012) 31–39.
33) L. Li, F. Liu, X. Jing, P. Ling and A. Li: Water Res. **45** (2011) 1177–1188.
34) S. Liu: Separ. Purif. Tech. **144** (2015) 80–89.
35) S. Liu: J. Colloid Interface Sci. **450** (2015) 224–238.
36) H. Lou, S. Li, X. Feng and X. Cao: Water Pract. Technol. **16** (2021) 1327–1342.
37) P.S. Pauletto, S.F. Lütke, G.L. Dotto and N.P.G. Salau: J. Mol. Liq. **336** (2021) 116203.
38) P. Tan, Y. Hu and Q. Bi: Colloids Surf. A Physicochem. Eng. Asp. **509** (2016) 56–64.
39) W.C. Tsai, M.D.G. de Luna, H.L.P. Bermillo-Arriesgado, C.M. Futalan, J.I. Colades and M.W. Wan: Int. J. Polym. Sci. **2016** (2016) 1608939.
40) S. Wang, T. Vincent, C. Faur and E. Guibal: Bioresour. Technol. **231** (2017) 26–35.
41) H. Xu, L. Tan, H. Dong, J. He, X. Liu, G. Qiu, Q. He and J. Xie: RSC Adv. **7** (2017) 32229–32235.
42) J. Yang, W. Wei, S. Pi, F. Ma, A. Li, D. Wu and J. Xing: Bioresour. Technol. **196** (2015) 533–539.
43) J. Zhang, X. Liu, X. Chen, J. Li and Z. Zhao: Hydrometallurgy **144–145** (2014) 77–85.
44) X.P. Zhang, F.Q. Liu, C.Q. Zhu, C. Xu, D. Chen, M.M. Wei, J. Liu, C.H. Li, C. Ling, A.M. Li and X.Z. You: RSC Adv. **5** (2015) 75985–75997.
45) J. Zhang and Y. Chen: RSC Adv. **6** (2016) 69370–69380.
46) Z. Zhao, J. Zhang, X. Chen, X. Liu, J. Li and W. Zhang: Hydrometallurgy **140** (2013) 120–127.
47) Y. Zhu, J. Hu and J. Wang: J. Hazard. Mater. **221–222** (2012) 155–161.
48) S. Lagergren: Handlingar **24** (1898) 1–39.
49) G. Blanchard, M. Maunaye and G. Martin: Water Res. **18** (1984) 1501–1507.
50) T. Gosset, J.-L.T. Trancart and D.R. Thévenot: Water Res. **20** (1986) 21–26.
51) Y.S. Ho and G. Mckay: Process Biochem. **34** (1999) 451–465.
52) J.P. Simonin: Chem. Eng. J. **300** (2016) 254–263.
53) S. Azizian: J. Colloid Interface Sci. **276** (2004) 47–52.
54) J. Zhang: Separ. Purif. Tech. **229** (2019) 115832.
55) C.H. Bolster and G.M. Hornberger: Soil Sci. Soc. Am. J. **71** (2007) 1796–1806.
56) E.C. Lima, F. Sher, A. Guleria, M.R. Saeb, I. Anastopoulos, H.N. Tran and A. Hosseini-Bandegharaei: J. Environ. Chem. Eng. **9** (2021) 104813.
57) S. Mallakpour and S. Rashidimoghadam: Polymer (Guildf.) **160** (2019) 115–125.
58) H. Moussout, H. Ahlafi, M. Aazza and H. Maghat: Karbala Int. J. Mod. Sci. **4** (2018) 244–254.
59) Y. Miyake, H. Ishida, S. Tanaka and S.D. Kolev: Chem. Eng. J. **218** (2013) 350–357.
60) A. Bleuzen, F. Foglia, E. Furet, L. Helm, A.E. Merbach and J. Weber: J. Am. Chem. Soc. **118** (1996) 12777–12787.
61) J.P. Hunt and R.A. Plane: J. Am. Chem. Soc. **76** (1954) 5960–5962.
62) F.-C. Xu, H.R. Krpuse and T.W. Swaddle: Inorg. Chem. **24** (1985) 267–270.
63) A. Liberti and A. Napoli: J. Inorg. Nucl. Chem. **33** (1971) 89–96.
64) I. Grenthe and G. Gårdhammar: Acta Chem. Scand. **26** (1972) 3207–3214.
65) A. Napoli: J. Inorg. Nucl. Chem. **34** (1972) 987–997.
66) H. Mizuochi, S. Shirakata, E. Kyuno and R. Tsuchiya: Bull. Chem. Soc. Jpn. **43** (1970) 397–400.

Appendix

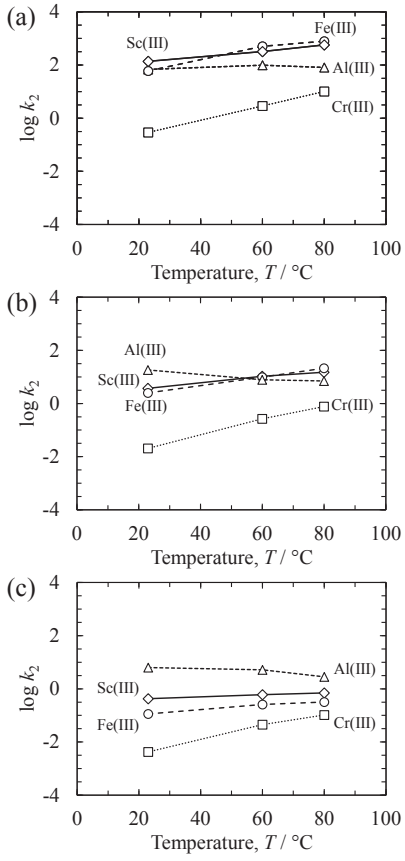

Fig. A1 Relationships between temperatures and pseudo second order rate constants of Sc(III), Cr(III), Al(III), and Fe(III); the initial concentrations of the ions were (a) 0.17, (b) 1.7, and (c) 17 mmol L^{-1}.

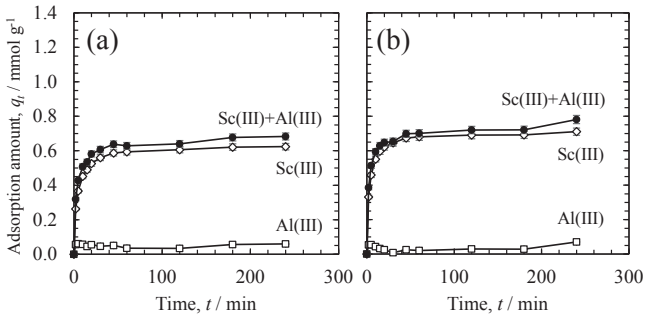

Fig. A2 Effects of time on adsorption of Sc(III) and Al(III) adsorption from the binary solution onto CR11 resin at (a) 25°C and (b) 60°C.

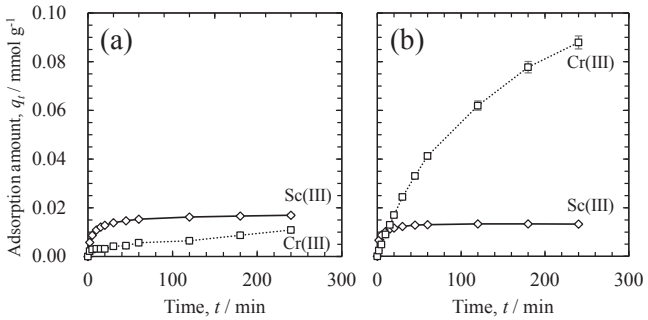

Fig. A3 Effects of time on adsorption of Sc(III) and Cr(III) adsorption from the synthetic solution onto CR11 resin at (a) 23°C and (b) 60°C.